Guided complex waves

Part 2. Relation to radiation patterns

T. Tamir, Ph.D., Associate Member, and Prof. A. A. Oliner, Ph.D.

Summary

The presence of complex waves in the near field of a source-excited plane homogeneous interface is shown to play an important role in determining certain features of the radiation field. A Kirchhoff–Huygens integration over the near field reveals that, whenever these complex waves are strongly excited, they account for peaks in the radiation pattern. Under unidirectional excitation, each complex wave yields a single peak at some oblique angle; for bi-directional excitation, either two peaks appear symmetrically located about a normal to the interface, or a single peak is present in this normal (broadside-on) direction. It is also shown that, when the complex wave is slowly decaying at the interface, the peaks occur close to the angle of definition θ_c for that wave. These angles of maximum radiation and the associated gain functions are expressed, in all these cases, in terms of the location in the steepest-descent plane of the pole corresponding to the complex wave. These features are also shown to be consistent with the radiation mechanism discussed in the companion paper, Part 1.

List of principal symbols

$a = \alpha_z/k$ = Normalized decay rate of a complex wave at the interface
$b = \beta_z/k$ = Normalized phase factor for a complex wave at the interface
$f(\kappa)$ = Complex amplitude function for the κ-mode
$G(x, z)$ = Total solution for the field in Cartesian co-ordinates
$G_p(x, z)$ = Pole contribution to $G(x, z)$
$G(r, \theta)$ = Total solution for the field in polar co-ordinates
$G_i(r, \theta)$ = Field obtained by means of a Kirchhoff–Huygens integration
$G_p(r, \theta)$ = Pole contribution to $G(r, \theta)$
$G_s(r, \theta)$ = Space-wave contribution to $G(r, \theta)$
$G_0(\phi_p)$ = Field contribution at the origin due to pole located at $\phi = \phi_p$
$k = \omega(\mu_0\epsilon_0)^{1/2}$ = Wave number of plane waves in free space
K = Gain function for $R_p(\theta)$
$R_p(\theta)$ = Radiation pattern due to a complex wave at the interface
$R_s(\theta)$ = Radiation pattern obtained from the steepest-descent result
r = Radial field co-ordinate
x, y, z = Cartesian field co-ordinates
$W(\phi_p)$ = Relative excitation coefficient
$Z_i(\kappa)$ = Impedance at the interface
α_z = Decay rate of complex wave at the interface
β_z = Phase shift of complex wave at the interface
ϵ_0 = Absolute permittivity of free space
$\zeta = \zeta_r + j\zeta_i$ = Wave number in the z-direction
$\zeta_p = \zeta_{pr} + j\zeta_{pi}$ = Location of a pole in the complex ζ-plane
η = Imaginary part of ϕ
η_p = Imaginary part of ϕ_p
θ = Angular field co-ordinate
θ_b = Angle of maximum radiation for a bi-directionally-excited complex wave
θ_c = Angle of definition for a pole contribution
θ_u = Angle of maximum radiation for a unidirectionally-excited complex wave
$\kappa = \kappa_r + j\kappa_i$ = Wave number in the x-direction
$\kappa_p = \kappa_{pr} + j\kappa_{pi}$ = Location of a pole in the complex κ-plane
μ_0 = Absolute permeability of free space
ξ = Real component of ϕ
ξ_p = Real component of ϕ_p
ρ = Distance from a field point to a point on the interface
ϕ = The steepest-descent complex variable
ϕ_p = Location of a pole in the complex ϕ-plane
$\psi(\rho)$ = A 2-dimensional Green's function
ω = Angular frequency

Paper 4093E, first received 19th March and in final form 7th August 1962
Dr. Tamir and Prof. Oliner are at the Microwave Research Institute, Polytechnic Institute of Brooklyn, New York

1 Introduction

In the companion paper,[1] which constitutes the first part of this study of complex waves guided by an interface, the waves themselves due to contributions from poles in the integral representation of the field were examined. It was shown that, although several types of such waves are possible, all these types are special cases of a general complex wave which possesses basic physical features common to all types. Thus, while some of these waves are spectral and satisfy a radiation condition, and others are improper, all of them occur in the form of an inhomogeneous plane wave which is propagated at some angle to the interface; also, all these waves are confined to a specified region of definition when the steepest-descent representation is used.

The first part of this study also dealt mainly with field configurations near the interface. Power considerations for this near field then showed that a complex wave is expected to account for a transfer of energy into the radiation field by means of the space wave and thus produce a peak in the radiation pattern of a specific source. The same physical reasoning also showed that this peak would arise at an angle which is close to the angle of definition θ_c of each complex wave in the steepest-descent representation. This power-flow feature has been known previously for improper complex waves; these are termed 'leaky waves' in the literature since they represented a leakage of energy from a specified structure into the radiation field. It was shown in the companion paper that this energy-transfer mechanism is also present for some of the proper complex waves which should, consequently, also be included in the category of leaky waves. For more details, reference should be made to the first part of this study.[1]

The present paper examines the far field in particular, and places it in a proper quantitative relationship to the near field investigated previously. For this purpose, a Kirchhoff–Huygens integration[2] over the near field is used, on the assumption that the complex wave provides the dominant contribution near the interface. It is then shown that peaks in the radiation pattern appear and are indeed intimately associated with the presence of poles in the integral representation and especially with their location in the steepest-descent plane. It is also demonstrated that the locations of these peaks in the radiation pattern are correctly predicted by the qualitative and physical considerations given previously whenever the decay rate of the complex wave is small. For large decay rates, however, the angle of maximum radiation may vary appreciably from θ_c. The radiation peak always occurs at an angle smaller than θ_c, i.e. nearer to the normal to the interface, and the effect of increasing the decay rate is to decrease the angle of maximum radiation until the peak occurs normal to the interface, at broadside.

Both uni- and bi-directional excitations of complex waves are considered, and it is shown that the peak under bi-directional excitation always appears at an angle smaller than that for unidirectional excitation. In fact, the peak for the unidirectional excitation always appears at an oblique angle, while the peak for the bi-directional excitation appears at broadside whenever a certain decay rate for the complex wave is exceeded. An expression for the gain of these peaks is also derived, and the results show that peaks nearer broadside are generally broader, while those nearer end fire are usually sharper.

It is noted that while some of these results have been known previously for non-modal waves from studies of leaky-wave aerials, all the results derived here are applicable to all types of complex guided wave, whether proper (spectral) or not.

In the present paper, use is made of certain of the results obtained in the first part[1] of this study; however, the need for extensive reference to the previous paper is avoided by the brief repetition in Section 2 herein of those features which are pertinent. Any discussion of those characteristics of complex waves which bear no direct relation to the radiation field is omitted from Section 2. The reader who wishes to clarify for himself certain additional features of the complex guided waves is therefore referred to the companion paper.[1]

In Section 3 the radiation field is dealt with, and its relation to the near field is discussed; in particular, suitable criteria are derived for establishing conditions under which the near field is dominated by a given complex wave. When these conditions are satisfied, a Kirchhoff–Huygens evaluation is justified whereby the far field is found by integrating over a complex-wave field at the interface only and disregarding the space-wave contribution altogether.

In Section 4, this Kirchhoff–Huygens procedure is applied, and the resulting radiation patterns are analysed. The radiation peaks and their associated gain functions are calculated for both uni- and bi-directional excitations. A discussion of the results obtained, as well as their relation to other aspects given in the previous paper, is also presented.

2 The field above an interface

The geometry considered is shown in Fig. 1, wherein a homogeneous, isotropic, infinite, plane interface is assumed to support a field excited by a source which may be located either above or below this interface. The boundary condition at the interface is expressed as an impedance function $Z_i(\kappa)$ which is specified for $x = 0$; it is assumed that $Z_i(\kappa)$ is independent of the co-ordinates y and z and is a function of the transverse wave number κ only. The medium above the

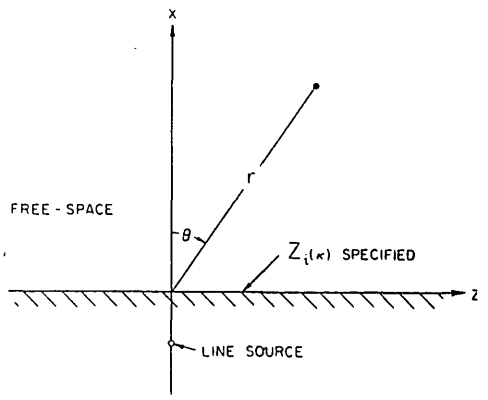

Fig. 1
Geometry of the plane interface

interface is free space and extends to infinity; only this region is considered, and the fields below the interface are not discussed. For convenience, it is assumed that the source is a magnetic or an electric line current at $z = 0$ and parallel to the y-axis; the problem is then two-dimensional and a solution is given by the Fourier transform

$$G(x, z) = \frac{1}{2\pi}\int_{-\infty}^{\infty} f(\kappa)\varepsilon^{j\kappa x}\varepsilon^{j\zeta z}d\zeta \quad x \geqslant 0 \quad . \quad . \quad (1)$$

with the integration being carried out along the real ζ-axis and a time dependence $\varepsilon^{j\omega t}$ being implied. The wave numbers κ and ζ, in the x- and z-directions respectively, are related by

$$\zeta = \pm\sqrt{(k^2 - \kappa^2)} \quad . \quad . \quad . \quad . \quad (2)$$

where $k = \omega\sqrt{(\mu_0\epsilon_0)}$ is the free-space wave number. Eqn. 2 necessitates a branch cut in the integral of eqn. 1; in addition, a radiation condition

$$\mathscr{I}\kappa > 0 \quad . \quad . \quad . \quad . \quad . \quad . \quad (3)$$

is required for the integral in eqn. 1 to converge properly at infinity. ($\mathscr{I}$ stands for 'the imaginary part of'.) The branch cut may then be so chosen that eqn. 3 is satisfied on the top sheet of a two-leafed Riemann complex plane; the bottom leaf of this plane then corresponds to $\mathscr{I} < 0$ and is therefore an improper sheet, so the integration is carried out along the entire real axis in the top sheet. To dispense with the branch cut, a transformation

$$\left.\begin{aligned}\zeta &= k\sin\phi\\ \kappa &= k\cos\phi\end{aligned}\right\} \quad . \quad . \quad . \quad . \quad . \quad . \quad (4)$$

is chosen, which plots the entire two-sheeted ζ-plane into a strip of width 2π in the complex ϕ-plane, as indicated in Fig. 2; in this Figure, the various quadrants of the ζ-plane divide into semi-infinite strips denoted by T (top sheet, proper) and B (bottom sheet, improper) and the quadrant number. The contour of integration is indicated by the path P in the Figure.

The integral in eqn. 1 may then be solved by means of a saddle-point technique which consists of deforming the path P into a steepest-descent path SDP given by

$$\cos(\xi - \theta)\cosh\eta = 1 \quad . \quad . \quad . \quad . \quad (5)$$

where ξ and η are the real and imaginary parts of ϕ, respectively, and θ is the saddle point. It can be shown that the contribution from the saddle point alone in such an integration is a space wave

$$G_s(r, \theta) \sim kF(\theta)\frac{\varepsilon^{j(kr-\pi/4)}}{\sqrt{(2\pi kr)}} \qquad \text{for } \theta \neq \pm\frac{\pi}{2}$$
$$. \quad . \quad . \quad . \quad (6)$$

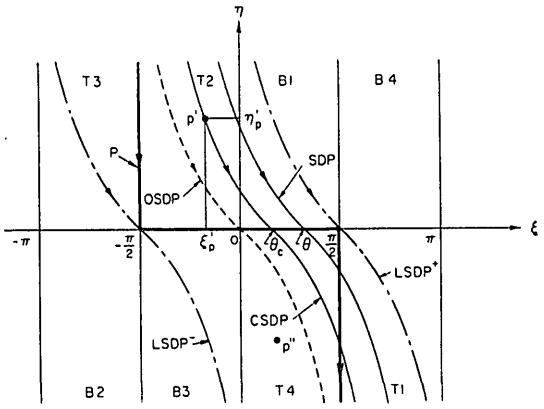

Fig. 2
Paths of integration in the steepest-descent ϕ-plane

$$G_s(r, \theta) = G_s(z) \sim \tfrac{1}{2} kF''\left(\pm\frac{\pi}{2}\right)\frac{\varepsilon^{j(k|z|-3\pi/4)}}{\sqrt{(2\pi|kz|^3)}} \quad \text{for } \theta \simeq \pm\frac{\pi}{2} \quad . \quad . \quad . \quad . \quad (7)$$

where
$$F(\phi) = f(\kappa)\cos\phi \quad . \quad . \quad . \quad . \quad (8)$$

and the $\sim$ sign denotes the asymptotic character of the above equations, which are accurate for large values of kr or $k|z|$. In addition, $f(\kappa)$ in eqn. 1 may contain poles; if a pole is located at $\phi_p = \xi_p + j\eta_p$ between the paths P and SDP, it then yields a contribution

$$G_p(r, \theta) = \pm jk\frac{[F(\phi_p)]^2}{F'(\phi_p)}\varepsilon^{jkr\cos(\phi_p-\theta)}\,U(\theta, \theta_c) \quad (9)$$

where the $\pm$ sign depends on the sense of the path essentially surrounding the pole; $U(\theta, \theta_c)$ is a step function which is unity if the relevant pole is captured by the steepest-descent path SDP and is zero otherwise. Poles contribute within angular regions characterized by the angle of definition θ_c, and the contribution then occurs within angles θ given by

$$\left.\begin{aligned} \theta_c \leqslant \theta \leqslant \pi/2 \quad &\text{if } a = \cos\xi_p \sinh\eta_p > 0 \\ -\pi/2 \leqslant \theta \leqslant \theta_c \quad &\text{if } a = \cos\xi_p \sinh\eta_p < 0 \end{aligned}\right\} \quad . \quad (10)$$

The total field is therefore given as

$$G(r, \theta) \sim G_s(r, \theta) + \sum_{p=1}^{N} G_p(x, z) \quad . \quad . \quad . \quad (11)$$

where it is assumed that a total of N poles contributes to the field.

An important feature of the steepest-descent representation given by eqn. 11 is that, in contrast to a spectral representation such as the one in eqn. 1, contributions may be obtained from poles even when these are located in the improper (bottom) leaf of the ζ-plane. Thus, an inspection of Fig. 2 shows that parts of the strips B1 and B3 may contain poles which can be captured by the steepest-descent curve and which then account for improper waves, denoted by the term 'leaky' in the literature.[3] These waves cannot exist by themselves but do constitute a valid portion of the total field; leaky waves have been identified experimentally[4] as distinct contributions which, together with the space wave, make up the total field.

It is noted that a more accurate expression for $G(r, \theta)$ would contain, in addition to the terms in eqn. 11, correction terms of the order of $(kr)^{-3/2}$ which occur in the asymptotic expansion of the space wave (the saddle-point contribution) as well as expressions containing error functions whenever the steepest-descent path passes near a pole. These additional terms are, however, omitted here, since they are unimportant in the evaluation of the far field, a fact that will be discussed further. It is also assumed that no branch cuts other than the one indicated in eqn. 2 are present in the integrand of eqn. 1; such branch cuts may also necessitate additional terms in the expression for $G(r, \theta)$.

3 The near field and the radiation pattern

3.1 Evaluation of the radiation field

The far field is given very accurately by eqn. 11 since, because of their asymptotic nature, these terms become more accurate as kr increases. In addition, the correction terms to eqn. 11 mentioned above then become insignificant, so that only the space wave and the pole contributions need be considered.

The location of the poles in the steepest-descent plane is given, in general, by complex values of ζ, κ and ϕ. This feature leads to a wave contribution which decays exponentially in all radial directions; such a decay exists whether the complex pole is proper (spectral) or improper. The only exception to this behaviour is the true surface wave which travels unattenuated along the interface; this wave is due to a pole which is characterized by $\phi_p = \pm\pi/2 + j\eta_p$. An inspection of eqn. 9 shows that such a pole contributes a wave which decays in all radial directions except that for which $r = z$, i.e. $\theta = \pm\pi/2$. Consequently, this type of pole contributes directly to the far field while the other types yield vanishingly small contributions; hence, only true surface waves, defined above, need be considered in connection with the far field in the summation term of eqn. 11.

The radiation field is usually regarded as that portion of the far field which corresponds to values of kr sufficiently large for the angular dependence of the field to be independent of r and to be properly characterized by a radiation pattern function $R(\theta)$. In agreement with the discussion above, the radiation field is given accurately by the space wave $G_s(r, \theta)$ of eqn. 6, everywhere except at, and very close to, the interface; in the latter region, the radiation field is obtained either by a space wave $G_s(z)$ given by eqn. 7 or, if true surface waves are present, by one or more terms of the form of $G_p(x, z)$, given in eqn. 9, with $\theta \simeq \pm\pi/2$, when the space-wave term of eqns. 6 and 7 is negligible. The radiation field is therefore characterized by a cylindrical wave which decays as $r^{-1/2}$ in all regions which are not too close to the interface. If a true surface wave is present, its field is a plane inhomogeneous wave which is independent of r along the interface; the space wave near the interface is then swamped out entirely in the radiation field by the surface wave.

The radiation pattern is therefore given accurately, from eqn. 6, by

$$R_s(\theta) = |F(\theta)|^2 \quad \text{for } \theta \neq \pm\pi/2 \quad . \quad . \quad (12)$$

For $\theta \simeq \pm\pi/2$, eqn. 12 is still valid if no true surface waves are present. Although $R_s(\theta)$ in eqn. 12 does not hold for $\theta \simeq \pm\pi/2$ if true surface waves are present, it is observed that in actual situations some losses always occur, so that any pole contribution decays exponentially; consequently, for sufficiently large r, eqn. 12 is correct for any angle $-\pi/2 \leqslant \theta \leqslant \pi/2$ in all physically realizable configurations of the type considered here. It is noted from eqns. 8 and 12 that $R_s(\theta)$ contains a $\cos^2\theta$ term which is consistent with the fact that as $\theta \to \pm\pi/2$, the first-order asymptotic result, which is proportional to $r^{-1/2}$, vanishes, and the next term, proportional to $r^{-3/2}$, must be considered.

3.2 Considerations for a Kirchhoff-Huygens evaluation

Although the radiation pattern is obtainable from eqn. 12, $F(\theta)$ may be found explicitly in only a few, usually idealized, configurations; in many actual cases, $F(\theta)$ is not available since the problem is either not amenable to a simple transverse interpretation in the form of an explicit $f(\kappa)$, or the evaluation of the integral representation by means of the steepest-descent procedure or otherwise becomes too complicated, with the result that $F(\theta)$ is not obtained in a simple analytical form. In many such cases, however, the near field is known either from actual measurements or, more often, by means of some simplified analytical considerations. Under these conditions, the radiation field may be evaluated by means of a Kirchhoff–Huygens technique[2] which consists essentially of an integration over this known near field.

Of particular interest is the situation in which complex guided waves are known to be present in the near field, especially when these waves are strongly excited. Then, although such waves are insignificant in the far field, owing to their exponential decay, they may nevertheless form the major contribution to the total field in the neighbourhood of the source and may even extend to considerable distances away from it. Such situations are already well known in leaky-wave aerials which involve improper complex waves.[3] More recently, the near fields of plasma slabs have been shown to contain both proper and improper complex waves;[5, 6] in these cases, the near field is given, to a first approximation, by an expression in the form of eqn. 9, provided that the space wave is negligible in that region.

It is important to recognize that the complete $f(\kappa)$, or $F(\phi)$ from eqn. 8, which must be known for the evaluation of the radiation pattern via eqn. 12, depends not only on the structure represented by the interface but also on the detailed description of the configuration in the immediate neighbourhood of the source. Very often, as with leaky-wave aerials, this source neighbourhood is very complicated, so that $f(\kappa)$ cannot be determined explicitly. The propagation characteristics of the complex wave guided by the interface do not depend on the source neighbourhood, however, but only on the properties of the interface, which can be expressed analytically in a relatively simple fashion. Thus, only the pole locations ϕ_p, or, alternatively, the singularities of $f(\kappa)$, rather than the complete function, will be determined; then only the amplitude of the function in eqn. 9 will not be known, and the resulting information is sufficient to permit a Kirchhoff–Huygens determination of the radiation pattern if the space wave is known to be negligible.

The omission of the space wave in certain cases has been justified by means of actual measurements,[7, 8] which showed that the near field conformed to a distribution of the type given by eqn. 9. Alternatively, if analytical results are available, conditions may be formulated to justify the validity of this approximation. The latter case is discussed below.

3.3 Criteria for a near field dominated by a complex guided wave

The Kirchhoff–Huygens integration procedure always involves a surface along which the field is prescribed. It is only natural that this surface be taken here as the interface itself; an additional advantage of this choice is that both the space wave and pole contributions correspond to particularly simple expressions along the interface since the θ dependence drops out there. It is also observed that the space wave decreases considerably faster with distance along the interface than with any other radial distance, as is evident when eqn. 6 is compared with eqn. 7; hence, if a complex pole contribution is strong relative to the space wave, this fact must be especially noticeable along the interface.

At the interface, the relevant paths of integration are those denoted by LSDP$^+$ (for $\theta = \pi/2$) and LSDP$^-$ (for $\theta = -\pi/2$). It is clear that only poles between these two paths need be considered; poles located elsewhere could contribute only correction terms to eqn. 11 and such terms are not considered here. The field at the interface due to a pole at $\phi_p = \xi_p + j\eta_p$ is obtained from eqn. 9 as

$$G_p(z) = \begin{cases} G_0(\phi_p)\varepsilon^{j\beta_z z}\varepsilon^{-\alpha_z z} & \text{if } \alpha_z z > 0 \\ 0 & \text{if } \alpha_z z < 0 \end{cases} \quad . \quad (13)$$

where

$$\left.\begin{aligned} \beta_z &= k \sin \xi_p \cosh \eta_p \\ \alpha_z &= k \cos \xi_p \sinh \eta_p \end{aligned}\right\} \quad . \quad . \quad . \quad . \quad (14)$$

and $G_0(\phi_p)$ is the excitation amplitude at the origin. The terms β_z and α_z are, respectively, the phase and the attenuation factors along the interface. For low decay rates, it is clear from eqn. 14 that either $\cos \xi_p$ or $\sinh \eta_p$ must be small; for such slowly attenuating waves, the corresponding poles must therefore be located close to either the $\xi = \pm \pi/2$ or the $\eta = 0$ axis.

It is evident from eqns. 14 that if the complex wave is to be comparable to the space wave in the near field, the decay rate $|\alpha_z|$ must be small. Noting that the near field corresponds to a region not too distant from the source, we can conveniently consider $kz \simeq 1$ in eqn. 13. It is then clear that if

$$|a| = \left|\frac{\alpha_z}{k}\right| = |\cos \xi_p \sinh \eta_p| \geqslant 1 \quad . \quad . \quad (15)$$

the wave is very strongly attenuated, since the amplitude decays by $1/\varepsilon$ in a travel of approximately one-sixth of a wavelength. The region defined by eqn. 15 is shown unshaded in Fig. 3; if poles exist in this region, their contribution to the total field may usually be disregarded since, even if strongly excited, these waves may be significant only within a very small region. Conversely, poles in the shaded region of Fig. 3 yield fields which are more slowly damped and may extend considerably away from the source.

The fact that a pole is located within the shaded region in Fig. 3 is not by itself sufficient to determine a strong complex-

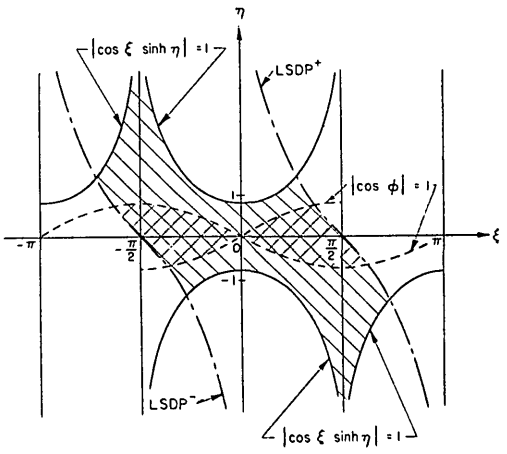

Fig. 3

Regions of pole contributions; the regions shown shaded may account for strong complex wave fields

wave contribution; it is also necessary that the excitation amplitude $G_0(\phi_p)$ be comparable to or larger than the excitation amplitude of the space wave. This latter condition may be expressed as

$$\left|\frac{G_p(z)}{G_s(z)}\right|^2 = W(\phi_p)\, H(a, z) \gg 1 \quad . \quad . \quad . \quad (16)$$

with the understanding that the inequality in eqn. 16 be satisfied over a sufficiently large distance from the origin. Using eqns. 7, 9 and 15 in conjunction with the above expression, we define the terms $W(\phi_p)$ and $H(a, z)$ as

$$W(\phi_p) = \left| \frac{[F(\phi_p)]^2}{F'(\phi_p)\, F''(\pi/2)} \right|^2 \quad . \quad . \quad . \quad (17)$$

$$H(a, z) = 2\pi |kz|^3 \varepsilon^{-2|akz|} \quad . \quad . \quad . \quad . \quad (18)$$

It is evident that $W(\phi_p)$ is a factor,* termed the *relative excitation coefficient*, which gives a measure of the power density of the complex wave at the interface, compared with that of the space wave; $H(a, z)$ then expresses the variation of this power ratio as a function of the decay rate a and the distance z from the origin. $H(a, z)$ is shown plotted in Fig. 4 for various values of a. It is noted that, for $|a| < 1$, $H(a, z)$ is larger than unity for an appreciable distance z; thus, for $|a| = 0{\cdot}2$, the complex-wave field is dominant over a distance exceeding four wavelengths and its amplitude may be more than 100 times that of the space wave. Hence, provided that $|a|$ is not too close to unity, the inequality in eqn. 16 is satisfied if

$$W(\phi_p) \gg 1 \quad |a| < 1 \quad . \quad . \quad . \quad . \quad (19)$$

If condition 19 is fulfilled, the near field at the interface is dominated by a complex wave; consequently, the combination of conditions $|a| < 1$ and $W(\phi_p) \gg 1$ serves as a sufficient criterion for establishing whether or not such a situation exists.

In actual leaky-wave aerials, parameter $|a|$ is commonly less than $0{\cdot}1$. This range has not been plotted in Fig. 4 because the resultant kz and $H(a, z)$ are then extremely large; for example, for $|a| = 0{\cdot}1$, $H(a, z)$ reaches over 1000. For such aerials, therefore, the complex wave is seen to be clearly dominant over large ranges of kz even if the relative excitation coefficient $W(\phi_p)$ is not greater than unity.

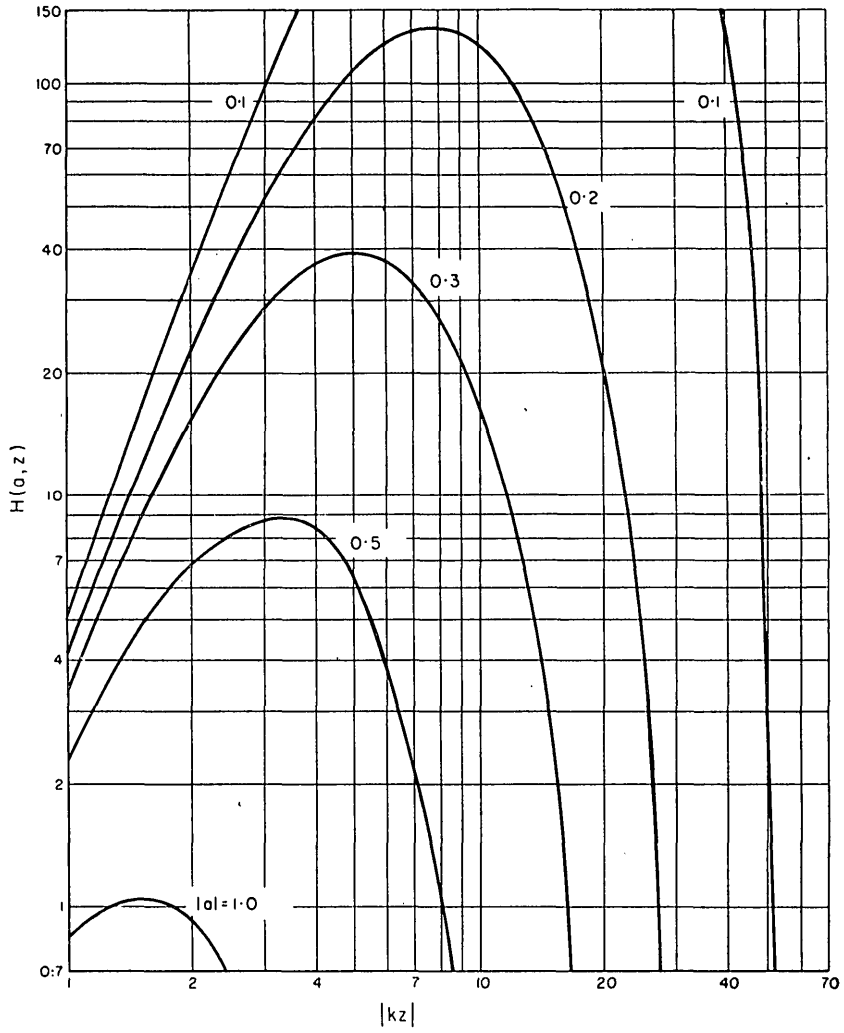

Fig. 4
Curves of $H(a, z)$ *against* $|kz|$ *for values of* $|a|$ *shown alongside curves*

4 The radiation pattern of a complex-wave distribution

4.1 The Kirchhoff–Huygens result

If condition 19 is fulfilled so that the complex wave indeed dominant in the near field, the far field may be evaluated by specifying the field of the complex wave itself at the interface. The geometry employed in such a calculation is indicated in Fig. 5; the field specified at the interface is then $G_p(z)$ as in eqn. 13, and the observation point P is that at which the far field $G_i(r, \theta)$ is to be evaluated. The subscript i in the latter indicates that this is a result obtained by means of an

* $W(\phi_p)$ as defined here differs by a factor of 2π from the same term in Reference 6

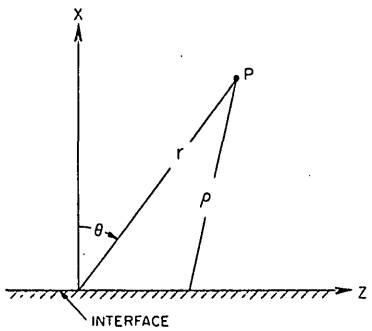

Fig. 5
Geometry for the Kirchhoff–Huygens integration

integration over the interface. The expression for $G_i(r, \theta)$ is then given by

$$G_i(r,\theta) = \int_{-\infty}^{\infty} \left[\psi(\rho) \frac{\partial G_p(z)}{\partial x} - G_p(z) \frac{\partial \psi(\rho)}{\partial x} \right] dz \quad . \quad (20)$$

where $\psi(\rho)$ is an appropriate 2-dimensional Green's function and ρ is the distance between a point z on the interface and the field point at P. It is recognized that, since the integration extends to infinite values of z, the complex wave distribution $G_p(z)$ does not represent the actual field for large z: although the condition 19 may be satisfied and thus correspond to a comparatively insignificant space wave $G_s(z)$ even up to a considerable distance from the source, the space-wave contribution will eventually, for sufficiently large z, yield the dominant contribution. However, this generally occurs only after the amplitudes of both $G_p(z)$ and $G_s(z)$ have become so small that their contributions to the integral in eqn. 20 may be disregarded.

Some ambiguity usually exists in specifying $\psi(\rho)$ since $\psi(\rho) + C\partial\psi(\rho)/\partial z$ may be required to vanish at the interface for a rather arbitrary value of the constant C. This may be resolved in the present case by noting that the exact asymptotic far-field result, expressed by eqns. 6 and 12, contains a $\cos\theta$ term; such a term is obtained from eqn. 20 by stipulating that $\psi(\rho)$ vanish at the interface ($\rho = 0$), i.e. that the interface act as a perfect reflector. Noting that the free-space two-dimensional Green's function is expressed by the Hankel function of the first kind $\frac{1}{4}jH_0^{(1)}(k\rho)$, one has

$$\psi(\rho) = \frac{j}{4}\left[H_0^{(1)}(k\rho_1) - H_0^{(1)}(k\rho_2) \right]_{\rho_2 \to \rho} \quad . \quad . \quad (21)$$

where ρ_1 and ρ_2 are distances from the point P to two points located symmetrically to the interface. Hence

$$\frac{\partial \psi(\rho)}{\partial x} = -\frac{jk}{2} H_1^{(1)}(k\rho) \frac{\partial \rho}{\partial x} \quad . \quad . \quad . \quad (22)$$

By introducing the last result into eqn. 20, one finds

$$G_i(r,\theta) = \frac{jk}{2} \int_{-\infty}^{\infty} H_1^{(1)}(k\rho)\, G_p(z) \frac{\partial \rho}{\partial x} dz \quad . \quad . \quad (23)$$

Since only the radiation field is of interest, r may be taken to be very large; in addition, since $G_p(z)$ contains an exponentially decaying term, only finite values of z yield significant contributions to the integral. One is therefore justified in assuming that $z \ll r$ in eqn. 23, so that

$$\rho \simeq r - z \sin\theta \quad . \quad . \quad . \quad . \quad . \quad (24)$$

Introducing eqn. 24 into eqn. 23, taking the Hankel-function approximation for large arguments, and employing the usual approximations which neglect second-order terms in the amplitude coefficients but retain these terms in the phase factor, one obtains

$$G_i(r,\theta) \simeq \frac{\varepsilon^{j(kr-\pi/4)}}{\sqrt{(2\pi kr)}} k \cos\theta \int_{-\infty}^{\infty} G_p(z) \varepsilon^{-jkz\sin\theta} dz \quad . \quad (25)$$

When the value of $G_p(z)$ is inserted into eqn. 25, the field may be readily evaluated by performing the integration. It is noted that this remaining integral is not a function of r and that the radial dependence of $G_i(r, \theta)$ is then identical to that of $G_s(r, \theta)$ in eqn. 6. In addition, the multiplier $\cos\theta$ has also been properly recovered, in agreement with the discussion preceding eqn. 21.

The radiation pattern may then be expressed as

$$R_p(\theta) \sim \left| k \int_{-\infty}^{\infty} G_p(z) \varepsilon^{-jkz\sin\theta} dz \right|^2 \cos^2\theta \quad . \quad . \quad (26)$$

where the subscript p in $R_p(\theta)$ indicates that this is a result derived by assuming a pole contribution at the interface.

It is realized that $G_p(z)$ must contain a properly decaying term for the integral in eqn. 26 to be defined; this reason, together with the condition containing the approximation expressed in eqn. 24, exclude from this discussion any non-attenuating surface waves, for which $\phi_p = \pm \pi/2 + j\eta_p$.

4.2 Unidirectional excitation

Owing to the $\pm$ signs in eqn. 2, any complex pole at $\kappa = \kappa_p$ necessarily corresponds to a pair of poles ζ_p and $-\zeta_p$ in the ζ-plane and hence to a pair of symmetrically located poles at ϕ_p and $-\phi_p$ in the steepest-descent plane, which are indicated by p' and p'' in Fig. 2. These poles correspond, respectively, to waves travelling in the positive and negative z-directions; at the interface, one such pole contributes for positive z only and the other pole in the pair contributes for negative z, as indicated by eqn. 13 or Fig. 2.

Although, in general, both poles are present, it is possible to excite only one of them by means of a unidirectional source; such excitation is common in many travelling-wave aerials.[4] The function to be used for $G_p(z)$ is then given by eqn. 13 which, when introduced in the integral of eqn. 26, yields

$$R_{pu}(\theta) = \left| \frac{\cos\theta}{\sin\phi_p - \sin\theta} \right|^2 \quad . \quad . \quad . \quad (27)$$

where the subscripts pu in $R_{pu}(\theta)$ designate a radiation pattern due to the unidirectional excitation of a wave corresponding to a pole p at $\phi = \phi_p$.

By taking the derivative of $R_{pu}(\theta)$ with respect to θ, one finds that there exists a single maximum

$$R_{pu}(\theta_u) = \frac{1}{\sinh^2 \eta_p} \quad . \quad . \quad . \quad . \quad . \quad (28)$$

where the angle of maximum radiation θ_u is given by

$$\sin\theta_u = \frac{\sin\xi_p}{\cosh\eta_p} \quad . \quad . \quad . \quad . \quad . \quad (29)$$

The radiation pattern $R_{pu}(\theta)$ therefore consists of a single lobe with a gain K_u (see Section 8) given by

$$K_u = \frac{\varepsilon^{|\eta_p|}}{\sinh|\eta_p|} \quad . \quad . \quad . \quad . \quad (30)$$

If the attenuation α_z of the complex wave is very small, then, unless $\xi_p \simeq \pi/2$, $|\eta_p|$ must also be very small; for $|\eta_p| \ll 1$, eqn. 30 becomes

$$K_u|_{|\eta_p| \ll 1} \simeq \frac{1}{|\eta_p|} \simeq \frac{\sqrt{(k^2 - \beta_z^2)}}{|\alpha_z|} \quad . \quad . \quad . \quad (31)$$

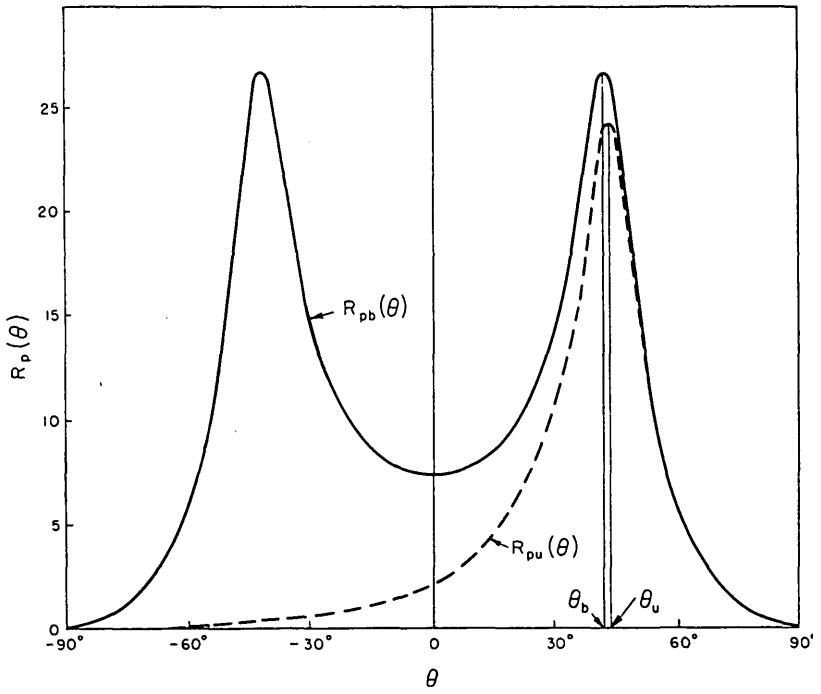

Fig. 6

Radiation patterns produced by a pole at $\phi_p = \pi/6 + 0{\cdot}2j$ ($|\cos \phi_p| < 1$)

—— Bi-directional excitation
---- Unidirectional excitation

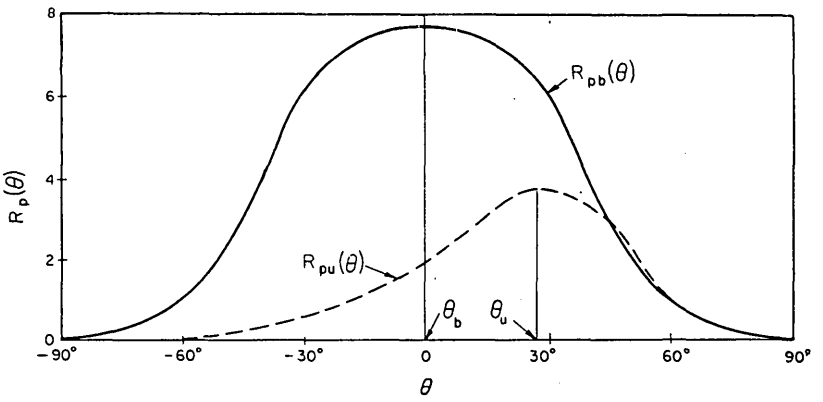

Fig. 7

Radiation patterns produced by a pole at $\phi_p = \pi/4 + 0{\cdot}5j$ ($|\cos \phi_p| > 1$)

—— Bi-directional excitation
---- Unidirectional excitation

From eqns. 28–31 it is therefore found that, in unidirectional excitation, there will always be a peak in the radiation pattern at some oblique angle; both this maximum and the gain of the radiation pattern are then functions of $|\eta_p|$ only, and they are therefore independent of ξ_p. Typical radiation patterns for this type of excitation are shown by the dashed curves in Figs. 6 and 7.

4.3 Bi-directional excitation

In the more general case, and especially for a line source as shown in Fig. 1, the excitation is bi-directional. The complex wave at the interface is then contributed by a pole pair ϕ_p, $-\phi_p$ which, with eqn. 13, yields a field

$$G_p(z) = \varepsilon^{jk|z|\sin\phi_p} \quad . \quad . \quad . \quad . \quad . \quad (32)$$

wherein the excitation coefficient $G_0(\phi_p)$ is again normalized to unity. Using this field in the integral of eqn. 26, one obtains

$$R_{pb}(\theta) = \left| \frac{2 \sin \phi_p \cos \theta}{\sin^2 \phi_p - \sin^2 \theta} \right|^2 \quad . \quad . \quad . \quad (33)$$

where the subscript b now indicates the bi-directional character of the relevant expressions. From the derivative of $R_{pb}(\theta)$, two distinct cases can be taken:

(*a*) $|\cos \phi_p| < 1$: The pole is therefore located in a region given by $\sinh |\eta_p| < \sin |\xi_p|$, shown cross-hatched in Fig. 3. The function $R_{pb}(\theta)$ then has a minimum at $\theta = 0$ and maxima given by

$$R_{pb}(\pm\theta_b) = \frac{\sin^2 \xi_p + \sinh^2 \eta_p}{\sin^2 \xi_p \sinh^2 \eta_p} \quad . \quad . \quad . \quad (34)$$

where the angles of maximum radiation $\theta = \pm \theta_b$ are obtained from

$$\cos \theta_b = |\cos \phi_p| = \sqrt{(\cosh^2 \eta_p - \sin^2 \xi_p)} \quad . \quad (35)$$

The gain for the radiation pattern is then

$$K_{b<} = \frac{\sin^2 \xi_p + \sinh^2 \eta_p}{4 \sinh^2 \xi_p \sinh^2 \eta_p} \sinh 2|\eta_p| \quad . \quad . \quad (36)$$

where the subscript $<$ indicates that $|\cos \phi_p| < 1$. For small attenuation, with small $|\eta_p|$ and $\xi_p \neq \pi/2$, eqn. 36 becomes, under the condition $\sinh |\eta_p| < \sin |\xi_p|$,

$$K_{b<}|_{|\eta_p| \ll 1} \simeq \frac{1}{2|\eta_p|} \simeq \frac{\sqrt{(k^2 - \beta_z^2)}}{2|\alpha_z|} \quad . \quad . \quad (37)$$

When eqns. 31 and 37 are compared, it is noted that the gain for bi-directional excitation is half that for unidirectional; the factor of one-half is due to the presence of two lobes, at $+\theta_b$ and $-\theta_b$, rather than a single lobe. Hence, when the decay of the complex wave is small, the gain for each separate radiation peak is the same whether bi-directional or unidirectional excitation is employed; this result is expected since the bi-directional case may be regarded as a superposition of two unidirectional fields, if the decay rate $|a|$ is small enough. Also, the gain is then independent of ξ_p and depends on η_p only, as indicated by eqns. 31 and 37.

A typical radiation pattern for this case is shown by the solid line in Fig. 6; it is noted that, because of the relatively low attenuation $|a|$, the unidirectional pattern is very similar to one of the bi-directional lobes.

(*b*) $|\cos \phi_p| > 1$, i.e. $\sinh |\eta_p| > \sin |\xi_p|$: The relevant pole at $\phi = \phi_p$ is then located outside the region shown cross-hatched in Fig. 3. The function $R_{pb}(\theta)$ now has a maximum only at $\theta = 0$ with

$$R_{pb}(0) = \frac{4}{\sin^2 \xi_p + \sinh^2 \eta_p} \quad . \quad . \quad . \quad (38)$$

with a resulting gain of

$$K_{b>} = \frac{\sinh 2|\eta_p|}{\sin^2 \xi_p + \sinh^2 \eta_p} \quad . \quad . \quad . \quad (39)$$

It is easy to show, for the same value of $|\eta_p|$ but appropriately different ξ_p, that

$$K_{b>} > K_{b<} \quad . \quad . \quad . \quad . \quad . \quad (40)$$

It is noted that, in contrast to the unidirectional case, the gain now depends on ξ_p in addition to η_p; also, it is seen for eqns. 36 and 39 that the gain is a function which, for constant η_p, decreases monotonically with $|\xi_p|$. Since eqn. 35 shows that the angle of maximum radiation $|\theta_b|$ increases with $|\xi_p|$, it follows that peaks at larger values of $|\theta_b|$ exhibit correspondingly smaller gains when $|\eta_p|$ is kept constant; in addition, eqn. 40 shows that if the peak occurs at broadside ($\theta_b = 0$), the gain is then larger than that for any oblique angle ($\theta_b \neq 0$) for the same value of $|\eta_p|$. It is realized, however, that poles which contribute broadside on ($|\cos \phi_p| > 1$) are generally located in regions in which $|\eta_p|$ is higher than it is for poles which contribute a peak at an oblique angle ($|\cos \phi_p| < 1$), as can be seen from Fig. 3. Since a high $|\eta_p|$ corresponds to a low gain, broadside-on peaks will generally appear to be low and spread out compared with most peaks at oblique angles.

A typical radiation pattern for this case is shown by the solid line in Fig. 7; it is noted that the bi-directional pattern now differs considerably from the unidirectional pattern produced by the same pole.

4.4 Radiation relations and considerations

When the unidirectional case is compared with the bi-directional case, it is seen from eqns. 29 and 35 that

$$\cosh \eta_p = \frac{\cos \theta_b}{\cos \theta_u} > 1 \quad . \quad . \quad . \quad . \quad (41)$$

so that the peak at θ_b for bi-directional excitation always occurs at a smaller angle, closer to the normal at the interface, than the peak at θ_u for the unidirectional case. It is also noted that, while θ_b may become zero, for $|\cos \phi_p| \geqslant 1$, θ_u can never vanish. These features are clearly seen in Figs. 6 and 7.

A relation between θ_u, θ_b, θ_c and ξ_p may be obtained by introducing eqn. 41 into eqn. 5 and setting $\phi = \phi_p$,

i.e. $$\cos (\xi_p - \theta_c) = \frac{\cos \theta_u}{\cos \theta_b} \quad . \quad . \quad . \quad . \quad (42)$$

It is clear from eqns. 41 and 42, and the use of eqns. 29 and 35, that, if $|\eta_p|$ is sufficiently small,

$$\theta_b \simeq \theta_u \simeq \xi_p \simeq \theta_c \quad |\eta_p| \ll 1 \quad . \quad . \quad . \quad (43)$$

Hence, if the decay rate α_z of the complex wave is sufficiently small, the radiation peaks for both bi-directional and unidirectional excitations occur at an angle close to the angle of definition of the complex wave.

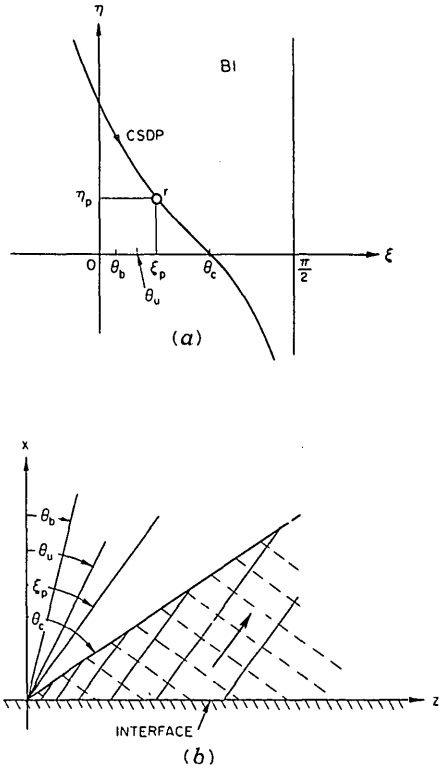

Fig. 8

Characteristic angles for an improper complex wave

(*a*) Location of an improper pole in the steepest-descent ϕ-plane
(*b*) Field contours for the wave above the interface

—— Equi-amplitude contours
---- Equi-phase contours
⟶ Direction of local power flow and increasing phase

In Fig. 2, a spectral complex pole p' is shown located in strip T2 and lying on the steepest-descent path CSDP. By inspection, it is evident that for such poles $|\theta_c|$ could be either greater than or less than $|\xi_p|$. However, for improper poles, located in strips B1 or B3, an additional relationship may be found. A pole located in strip B1 is shown in Fig. 8(*a*); from the Figure, and from eqns. 41 and 42, it is seen that

$$|\theta_b| < |\theta_u| < |\xi_p| < |\theta_c| \quad . \quad . \quad . \quad . \quad (44)$$

In the limit of negligibly small attenuation for the improper complex wave, eqn. 44 reduces to eqn. 43, as expected. The angular relationships displayed by eqn. 44 are illustrated in Fig. 8(*b*).

In the companion paper,[1] it was shown from qualitative and physical considerations that a strongly excited complex wave is expected to account for a radiation peak at an angle close to the definition angle θ_c. This result was obtained by noting that complex waves transferred energy across the boundary defined by θ_c into the space wave and thence into the radiation field. Since the space wave travels radially, a radiation peak at or close to θ_c was expected. An illustration of these considerations is offered in Fig. 8(*b*) for an improper complex wave.

It is seen from eqn. 43 that the above expected result is verified exactly in the limit of vanishingly small decay rate for the complex wave. When complex waves with non-negligible attenuation constants are considered, the radiation peaks still occur close to θ_c if $|\eta_p|$ is small, but may differ appreciably from θ_c if $|\eta_p|$ is large.

It is emphasized that although only one complex wave at a time was considered thoughout this paper, actual situations may require more than one pole in the integral representation of the field. Then, more than one complex wave may be strongly excited and each of them will account for a peak in the radiation pattern. Consequently, the angular location of these peaks may be predicted correctly from a knowledge of the location of the poles in the steepest-descent plane. As an example, Fig. 9 shows a radiation pattern obtained for a plasma slab;[6] all the peaks are correctly accounted for by four major contributing complex wave poles. Additional poles are also present but they comply with $|\cos \phi_p| > 1$, so that they contribute to the radiation field mainly in a direction normal to the interface.

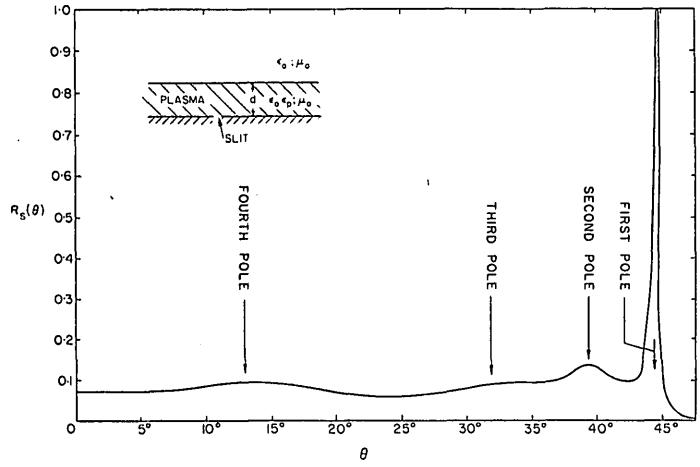

Fig. 9

Radiation pattern for a grounded plasma slab excited by a slit ($\epsilon_p = 0{\cdot}5$; $d/\lambda = 1{\cdot}414$)

The pattern shown is an exact asymptotic one obtained by means of the steepest-descent result $R_s(0)$. The angles for which peaks are expected owing to the presence of complex poles are indicated by arrows

A comparison of the radiation patterns obtained from a direct saddle-point evaluation, using eqn. 12, and via a Kirchhoff–Huygens integration, using eqn. 33, is presented in Fig. 10. The data shown correspond to a slit-excited plasma sheet over a ground plane;[6] the near field for this structure, for the parameters chosen, is indeed dominated by a single complex guided wave. It is seen that excellent agreement is obtained between the two patterns, thus verifying the validity of the integration technique and illustrating its usefulness.

The validity of the integration has also been demonstrated for a particular leaky-wave aerial[9] by a careful comparison with measurement. The measured radiation patterns were found to agree extremely well with the patterns computed by assuming that only a single complex wave was present in the near field.

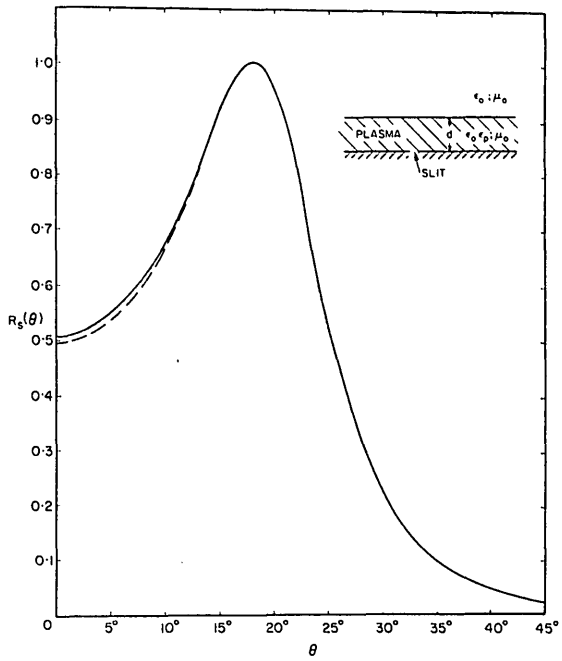

Fig. 10

Radiation pattern for a grounded plasma slab excited by a slit ($\epsilon_p = 0{\cdot}1$; $d/\lambda = 0{\cdot}168$)

---- Radiation pattern $R_{pb}(\theta)$
—— Exact asymptotic pattern $R_s(\theta)$

5 Conclusion

The radiation pattern of a line source in the neighbourhood of a plane homogeneous interface has been shown to be strongly related to the presence of poles in the integral representation of the field whenever the complex guided waves due to these poles are strongly excited. The peaks in the radiation pattern are especially sharp whenever the complex waves producing them decay slowly along the interface.

The angular location of these peaks and their gain have been shown to depend only on the location of the poles in the steepest-descent plane. A knowledge of the presence of such poles, together with their location, enables one to predict the shape of a resulting radiation pattern, wherein each peak is associated with a particular pole. In this fashion, the radiation pattern of certain aerials may be realized by designing a suitable configuration which is characterized by complex poles due to free resonances in the transverse network representing the configuration. The location of such poles in the steepest-descent plane is usually determined by parameters involving the geometry, the frequency or the physical characteristics of the media employed; hence, by varying these parameters suitably, the location of the poles may be chosen in such a manner as to realize a desired radiation pattern. The usefulness of such a procedure has already been recognized in leaky-wave aerials, and the present paper indicates that similarly rewarding possibilities are obtainable with a more general class of guided waves.

6 Acknowledgment

The study reported in the paper was sponsored by the U.S. Air Force Cambridge Research Laboratories, under contract No. AF 19(604)–7499.

7 References

1 TAMIR, T., and OLINER, A. A.: 'Complex guided waves: Part I—Fields at an interface' (see page 310)
2 STRATTON, J. A.: 'Electromagnetic theory' (McGraw-Hill, 1941), p. 460
3 ZUCKER, F. J.: 'Surface- and leaky-wave antennas', in Jasik, Henry (Ed.), 'Antenna Engineering Handbook' (McGraw-Hill, 1961), Ch. 16
4 CASSEDY, E. S., and COHN, M.: 'On the existence of leaky waves due to a line source above a grounded dielectric slab', *Trans Inst. Radio Engrs*, 1961, **MTT-9**, p. 243
5 TAMIR, T., and OLINER, A. A.: 'The spectrum of electromagnetic waves guided by a plasma layer', *Proc. Inst. Radio Engrs* (to be published)
6 TAMIR, T., and OLINER, A. A.: 'The influence of complex waves on the radiation field on a slot-excited plasma layer', *Trans Inst. Radio Engrs*, 1962, **AP-10**, p. 55
7 HINES, J. N., RUMSEY, V. H., and WALTER, C. H.: 'Traveling-wave slot antennas', *Proc. Inst. Radio Engrs*, 1953, **41**, p. 1624
8 GOLDSTONE, L. O., and OLINER, A. A.: 'Leaky wave antennas: Part I—rectangular waveguides', *Trans Inst. Radio Engrs*, 1959, **AP-7**, p. 307
9 HONEY, R. C.: 'A flush-mounted leaky wave antenna with predictable patterns', *ibid.*, p. 320

8 Appendix: derivation of gain functions

For the cases considered here, the gain for the radiation patterns is given by

$$K = \frac{\pi R_p(\theta_{max})}{\int_{-\pi/2}^{\pi/2} R_p(\theta)d\theta} \quad . \quad . \quad . \quad . \quad . \quad (45)$$

where θ_{max} is the angle of the peak, i.e. either θ_n or θ_b, for the unidirectional and bi-directional cases, respectively. The integral in the denominator is then evaluated as follows:

(*a*) Unidirectional:

By substituting for $R_p(\theta)$ from eqn. 27, one obtains for the integral of eqn. 45

$$I_u = \int_{-\pi/2}^{\pi/2} \frac{\cos^2\theta\, d\theta}{(\sin\theta - \sin\phi_p)(\sin\theta - \sin\phi_p^*)}$$

$$= \int_{-\pi/2}^{\pi/2} \left[\frac{\cos^2\phi_p}{2ja(\sin\theta - \sin\phi_p)} - \frac{\cos^2\phi_p^*}{2ja(\sin\theta - \sin\phi_p^*)} - 1 \right] d\theta \quad . \quad . \quad . \quad . \quad (46)$$

where the integration is taken along real values of θ, the asterisk stands for the complex conjugate and, for brevity,

$$\sin\phi_p = b + ja \quad . \quad . \quad . \quad . \quad . \quad (47)$$

with a and b purely real. Because of the periodicity of its functions, eqn. 47 may be expressed as

$$I_u + \pi = \frac{1}{2a}\mathscr{I}\int_0^{2\pi} \frac{\cos^2\phi_p d\theta}{\sin\theta - \sin\phi_p} \quad . \quad . \quad . \quad (48)$$

After a transformation

$$z = e^{j\theta} \quad . \quad . \quad . \quad . \quad . \quad . \quad . \quad (49)$$

eqn. 48 yields

$$I_u + \pi = \frac{1}{a}\mathscr{I}\oint \frac{\cos^2\phi_p dz}{z^2 - 2jz\sin\phi_p - 1} \quad . \quad . \quad (50)$$

where the integration is along the unit circle centred at the origin of the complex z-plane. The only singularities of the integrand are two simple poles at $z = \varepsilon^{j\phi_p}$ and $z = -\varepsilon^{-j\phi_p}$. However, only one of these poles is within the unit circle and is located at $z = \pm\varepsilon^{\pm j\phi_p}$ as $\eta_p \gtrless 0$, respectively. From the appropriate residue, it is obtained that

$$I_u + \pi = \frac{1}{a}\mathscr{I}(\pm 2\pi j\cos\phi_p)$$

$$= \pm\pi\coth\eta_p = \pi\coth|\eta_p| \quad (51)$$

so that

$$I_u = \pi(\coth|\eta_p| - 1) \quad . \quad . \quad . \quad (52)$$

When eqn. 52 is introduced and eqn. 28 is substituted for $R_p(\theta_{max})$ in eqn. 45, the gain obtained is that given by eqn. 30.

(*b*) Bi-directional:

Here, eqn. 33 expresses the appropriate relation for $R_p(\theta)$; the integral in the denominator of eqn. 45 then becomes

$$I_b = 4|\sin^2\phi_p| \int_{-\pi/2}^{\pi/2} \frac{\cos^2\theta d\theta}{(\sin^2\theta - \sin^2\phi_p)(\sin^2\theta - \sin^2\phi_p^*)} \quad (53)$$

which, from eqn. 47, may be expressed as

$$I_b = \frac{|\sin^2\phi_p|}{2ab}\mathscr{I}\left[\frac{1}{\sin\phi_p}\int_0^{2\pi}\left(\frac{\cos^2\phi_p}{\sin\theta - \sin\phi_p} - \frac{\cos^2\phi_p}{\sin\theta + \sin\phi_p}\right)d\theta\right] \quad (54)$$

It is noted that the integrand has the same form as that in eqn. 48 whose solution was given in eqn. 51; substituting the latter result into eqn. 54, one obtains

$$I_b = \frac{|\sin^2\phi_p|}{2ab}\mathscr{I}(\pm 4\pi j\cot\phi_p) = \pm\frac{4\pi}{\sinh 2\eta} = \frac{4\pi}{\sinh 2|\eta|} \quad . \quad . \quad . \quad . \quad (55)$$

Upon introduction of eqn. 55 and substitution of eqn. 34 or 38 for $R_p(\theta_{max})$ in eqn. 45, the gain obtained is given by eqns. 36 and 39, respectively.